Int. J. Electrochem. Sci., 12 **(2017)** 8399 – 8410, doi: 10.20964/2017.09.61

International Journal of
ELECTROCHEMICAL
SCIENCE
www.electrochemsci.org

Short Communication

Uranium Dissolution Behavior in LiCl-KCl Molten Salts

Sung-Jai Lee, Gha-Young Kim[*]

Pyroprocess Technology Division, Korea Atomic Energy Research Institute, 989-111 Daedeok-daero, Yuseong-gu, Daejeon, 34057, Republic of Korea
[*]E-mail: gkim@kaeri.re.kr

Received: 14 June 2017 / *Accepted:* 28 July 2017 / *Published:* 13 August 2017

Uranium (U) dissolution behavior at an anode during electrorefining was investigated by employing the potentiodynamic polarization method, galvanostatic potential transient technique, AC impedance spectroscopy, and potentiostatic current transient technique. For this purpose, a U pellet of diameter 8 mm and length 10 mm was used as the working electrode. From the quantitative analyses of the polarization curve and potential transient curves, the kinetic parameters governing the U dissolution reaction, such as the exchange current density and diffusivity of U ions in the LiCl-KCl fused salt, were determined. From the impedance spectra and anodic current transient curves obtained at various applied potentials, it was confirmed that the interfacial charge transfer for U dissolution is kinetically coupled with diffusion through the electrolyte. In addition, we found that AC impedance spectroscopy was more useful compared to the potentiostatic current transient technique in the presence of a large uncompensated ohmic potential drop.

Keywords: Pyroprocessing, Electrorefining, Uranium dissolution, Dissolution mechanism, Kinetic parameter

1. INTRODUCTION

For several decades, the pyrometallurgical treatment of spent nuclear fuel (SNF) has been extensively investigated because of its relatively low processing cost as well as its proliferation resistance of the nuclear fuel cycle [1-3]. Recently, the recovery of long-lived nuclides is awakening new interest in the fuel cycle process, since the geological disposal of high-level waste is facing significant difficulties in obtaining public acceptance, and, at the same time, the recovered uranium (U) and transuranic (TRU) elements can be re-utilized as a fuel source [4,5].

The electrorefining process is key to pyroprocessing of SNF and determines the efficiency of the overall process because a large amount of U in the SNF is recovered at this stage. Therefore, many

researchers have studied the electrorefining process to enhance throughput for practical applications. For example, the Argonne National Laboratory (ANL, US) has developed an electrorefiner with multiple cathodes [5], and the Central Research Institute of Electric Power Industry (CRIEPI, Japan) adopted a scraper system [6]. Much of the research has focused on the cathodic part [7-9], but relatively little attention has been paid to the mechanism of anodic dissolution during electrorefining.

Under these circumstances, it is necessary to elucidate the mechanism of the U dissolution and deposition reactions to achieve higher performance and efficiency of the electrorefiner. The fuel component such as U is dissolved from the anode basket in the molten salt electrolyte through the anodic reaction, and can then be recovered on the cathode via deposition. A recent study reported that the anodic process predominantly controls the overall electrorefining rate [10], but the qualitative results made it very difficult to completely grasp the kinetic properties of the anodic process. Thus, a more in-depth study is highly desirable.

In this respect, the present work aims to elucidate the mechanism of U dissolution during electrorefining using various electrochemical techniques such as AC impedance spectroscopy and a potentiostatic current transient. In this study, the kinetic parameters governing the U dissolution reaction were determined, followed by investigation of the dissolution mechanism of the U pellet electrode.

2. EXPERIMENTAL

2.1. Cell configuration

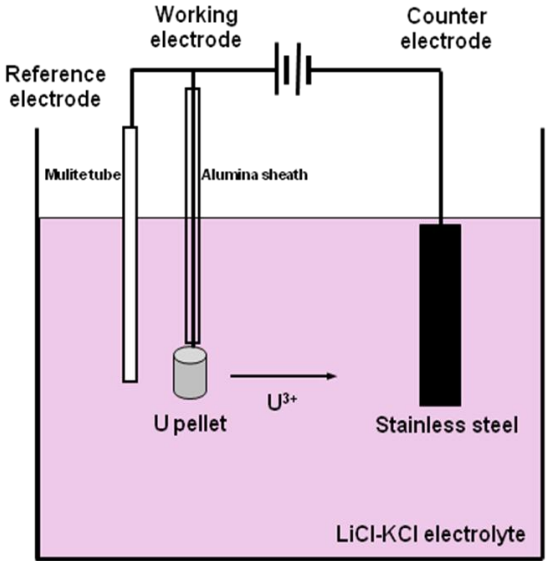

Figure 1. Schematic representation of the electrochemical cell used in this work.

A three-electrode electrochemical cell was employed for electrochemical measurements, as shown in Fig. 1. In this work, a U pellet 8 mm in diameter and 10 mm in length was used as the working electrode to investigate U dissolution behavior. The electrochemically active area of the U

pellet was 3.52 cm^2. A stainless steel rod and Ag/AgCl (1 wt%) were used as the counter and reference electrodes, respectively. A high purity LiCl–KCl eutectic salt (41.5–58.2 mol%, Sigma-Aldrich) was used as an electrolyte. All chemicals and apparatuses were handled in a glove box in which both the oxygen and moisture content were maintained below 10 ppm in an argon atmosphere.

2.2. Electrochemical measurements

An insulated stainless steel cell was placed in a stainless steel thermowell, which was heated externally with an electric furnace attached to the bottom surface of the glove box. The temperature was maintained at 500 °C. Prior to electrochemical experiments, uranium tri-chloride (UCl_3) was incorporated into the molten LiCl–KCl salt by an oxidation reaction between the uranium metal in the anode basket and the $CdCl_2$ in the salt giving a resulting concentration of 0.5 M UCl_3 in the salt. The electrode was cycled 10 times from -1.5 to 0 V (Ag/AgCl) at a scan rate of 100 mV s^{-1} to activate the working electrode.

All electrochemical experiments were performed with a ModuLab Electrochemical Test System (AMETEK Solartron). To evaluate the kinetic parameters of U dissolution, potentiodynamic polarization curves were measured at a potential range of −1.5 to 0 V (Ag/AgCl) with a scan rate of 10 mV s^{-1}. The galvanostatic potential transient curve was measured by applying a constant current of either 0.6 or 0.8 A. Impedance spectra were measured at applied potentials ranging from -1.3 to 1.0 V (Ag/AgCl) by applying an AC amplitude of 10 mV_{RMS} over a frequency range of 100 kHz to 1 Hz. Here, ten data points of the measured impedance spectra were taken every decade of the logarithmic frequency. Potentiostatic current transients were measured by jumping the electrode potential from the open circuit potential (OCP) to various potentials from -1.3 to 1.0 V (Ag/AgCl).

3. RESULTS AND DISCUSSION

3.1. Determination of kinetic parameters

In general, the potentiodynamic polarization curve is very important to understand the electrochemical properties of electrochemical reactions [11]. In the present work, the polarization curve was measured with the U pellet electrode to determine the kinetic parameters for the U dissolution reaction. The resulting curve is plotted with linear and semi-logarithmic scales in Figs. 2(a) and (b), respectively.

The current–potential relationship can be theoretically calculated from the Butler-Volmer equation as follows [12]:

$$i = i_o\left[\exp\left(\frac{-\alpha zF}{RT}\eta\right) - \exp\left(\frac{(1-\alpha)zF}{RT}\eta\right)\right] \quad (1)$$

where i represents the current density; i_o, the exchange current density; α, the cathodic transfer coefficient; z, the number of transferred electrons for U dissolution; F, a Faraday constant of 96,485 C

mol^{-1}; R , the gas constant; T, temperature in K; and η, the overpotential, which indicates the difference between the electrode potential and the OCP.

The kinetic parameters were quantitatively determined by the following two methods. First, for sufficiently small values of η, Eq. (1) can be expressed as

$$i = \frac{zFi_o}{RT}\eta = \frac{\eta}{R_p} \quad (2)$$

According to Eq. (2), the current is linearly proportional to the overpotential in a narrow potential range near the OCP. In Fig. 2(a), the OCP for the U pellet electrode was −1.341 V (Ag/AgCl), and the value of i_o was calculated to be 1.06×10^{-2} A cm^{-2} from the slope of the linear part of the polarization curve.

Second, for large values of η, one of the bracketed terms in Eq. (1) becomes negligible. In this work, we considered the U dissolution reaction, and thus Eq. (1) can be expressed at large positive overpotentials as follows:

$$i = i_o \exp\left(\frac{(1-\alpha)zF}{RT}\eta\right) \quad (3)$$

From the plot of log i vs. η, which is generally known as a Tafel slope, the values of i_o and α were determined to be 1.98×10^{-2} A cm^{-2} and 0.12, respectively. Here, it is noteworthy that the resulting values of i_o obtained from two different methods are almost the same.

In the field of electrochemistry, the diffusivity of the electroactive species is one of the most important parameters governing electrochemical reactions. To determine the diffusion coefficient of U ions, the galvanostatic potential transient curve was measured on the U pellet electrode by applying a constant current of 0.6 or 0.8 A.

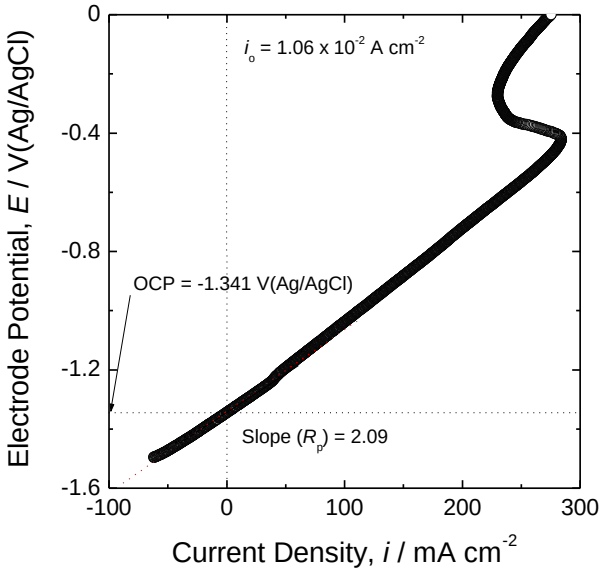

(a)

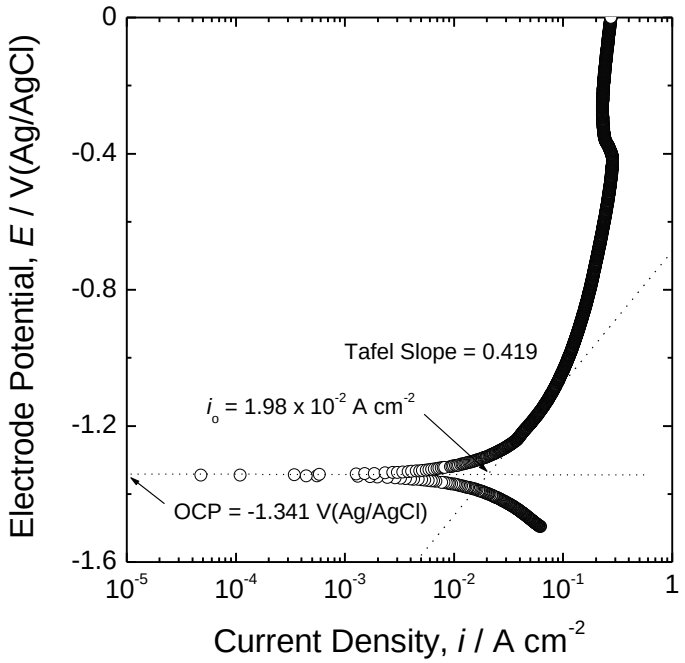

(b)

Figure 2. Potentiodynamic polarization curves on (a) linear and (b) semi-logarithmic scales measured from the U pellet electrode using a potential scan range from -1.5 to 0 V (Ag/AgCl) with a scan rate of 10 mV s^{-1}.

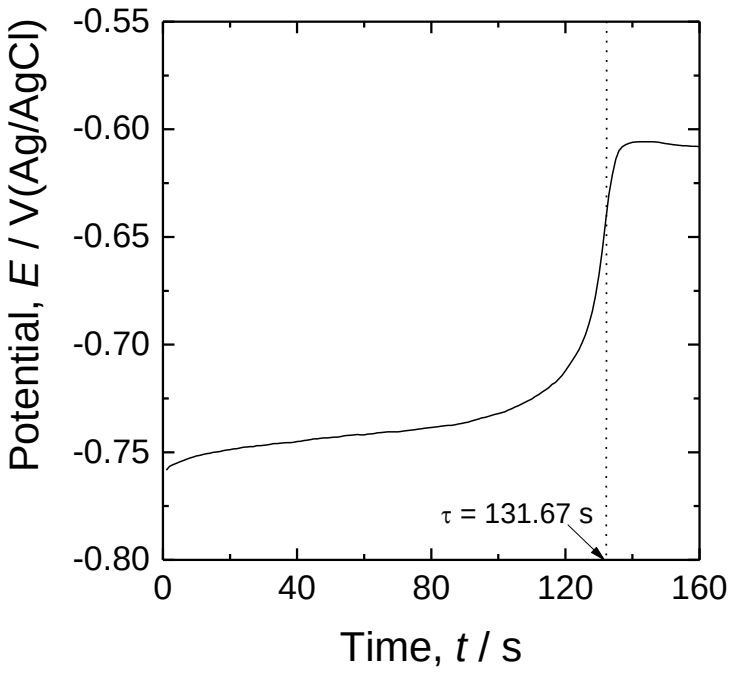

(a)

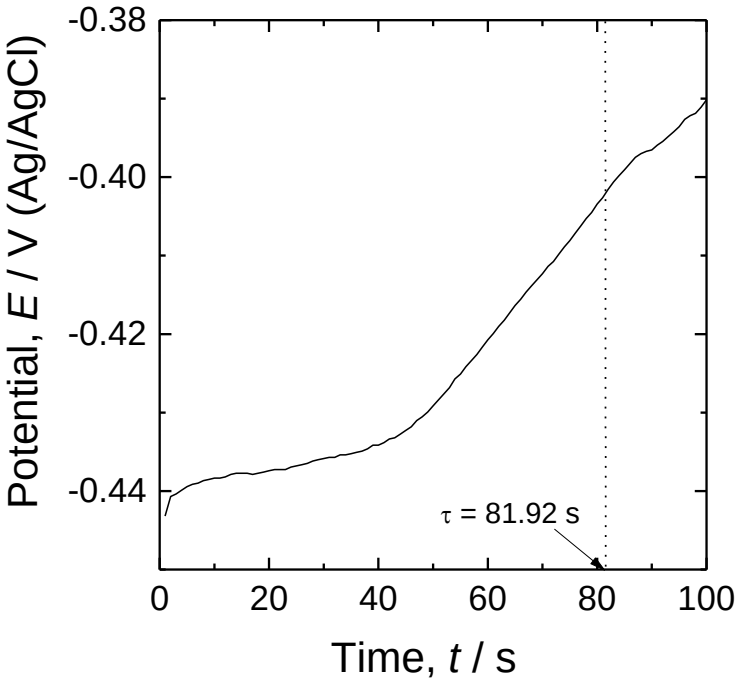

(b)

Figure 3. Potential transient curves obtained from the U pellet electrode at a constant current of (a) 0.6 A and (b) 0.8 A.

Here, it should be stressed that we applied relatively large currents in order to determine the diffusivity using diffusion-controlled electrochemistry [12]. The resulting curves are plotted in Figs. 3(a) and (b). In Fig. 3, the potential transient showed a typical shape, in which the potential gradually increased and then drastically jumped to a higher potential at the transition time.

To analyze the potential transient curve quantitatively, we applied the Sand equation as follows [12]:

$$\frac{i\tau^{1/2}}{c_{U^{3+}}} = \frac{zFD_{U^{3+}}^{1/2}\pi^{1/2}}{2} \quad (4)$$

where τ is the transition time, $c_{U^{3+}}$ is the bulk concentration of U ions, and $D_{U^{3+}}$ is the diffusion coefficient of U ions. Considering a constant U ion concentration of 0.5 M, the values of $D_{U^{3+}}$ were calculated from Eq. (4) to be 2.33×10^{-4} cm^2 s^{-1} and 2.57×10^{-4} cm^2 s^{-1} by taking the values of τ as 131.67 s and 81.92 s, respectively.

This value is quite similar to the experimental results previously reported by some researchers [2,8], but slightly larger than those reported by other researchers [13,14]. The slight discrepancy between the reported diffusion coefficients may be attributable to the high ion concentration and/or larger surface area originating from the surface roughness of the working electrode.

3.2. Determination of dissolution mechanism

AC impedance spectroscopy is an exceptionally powerful tool and has widely been used to identify various reaction steps, and ascertain the rate-determining step, as it may separately quantify the dynamics of several electrode processes with different relaxation times [15].

Fig. 4(a) gives the Nyquist plots of the impedance spectra experimentally measured on the U pellet electrode at different applied potentials of -1.3 to -1.0 V (Ag/AgCl). All measured impedance spectra consist of a depressed arc at high frequencies and a straight line inclined at a constant phase angle of −45° to the real axis, which is generally called the 'Warburg impedance', at low frequencies.

The first arc is mainly caused by the charge transfer reaction at the electrode/electrolyte interface [16,17], and the Warburg impedance is closely associated with the semi-infinite diffusion of the electroactive species through the electrolyte. The Warburg impedance, Z_W, is given as [18]

$$Z_W = R_W \frac{\coth\sqrt{j\omega/\omega_o}}{\sqrt{j\omega/\omega_o}} \quad (5)$$

where R_W is the diffusion resistance j is the unit of complex numbers, i.e. $\sqrt{-1}$, ω is the angular frequency and ω_o is the reciprocal of the diffusion time constant for finite diffusion.

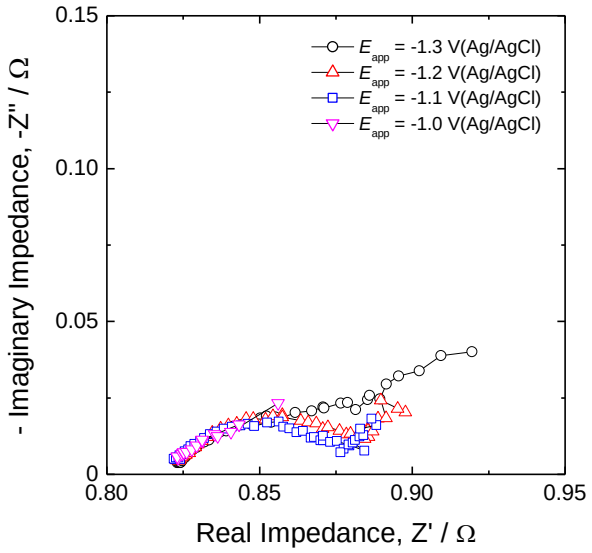

(a)

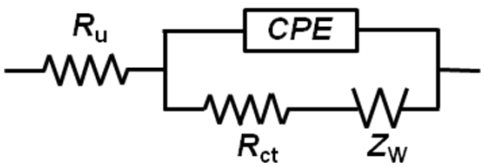

(b)

Figure 4. (a) Nyquist plots of the impedance spectra measured on the U pellet electrode at various applied potentials of -1.3 to -1.0 V (Ag/AgCl), and (b) the equivalent circuit used for analysis of the measured impedance spectra.

To determine the values of resistance and capacitance, the measured impedance spectra were analyzed using the complex nonlinear least squares (CNLS) fitting method [19] on the basis of the equivalent circuit, which is given in Fig. 4(b). Here, R_u is the uncompensated ohmic resistance, and R_{ct} and *CPE* represent the resistance and constant phase element associated with the charge transfer reaction and interfacial double layer charging, respectively.

The values of R_u, R_{ct}, and R_W were quantitatively determined from the CNLS fitting of the experimental impedance spectra, and their resulting values are plotted as a function of the electrode potential in Fig. 5. In Fig. 5, as the overpotential increases, the value of R_{ct} decreases, but the values of R_u and R_W remain nearly constant regardless of the overpotential. This result demonstrates that the value of R_{ct} is strongly dependent upon the overpotential, but R_W and R_u are potential-invariant.

By considering only the reaction resistances of R_{ct} and R_W, the values of R_{ct} and R_W are comparable with each other. Hence, it is reasonable to state that the charge transfer reaction and diffusion simultaneously affect the overall U dissolution reaction over the entire potential range, and the effect of R_{ct} on the overall dissolution resistance is reduced with an increase in overpotential. In addition, the value of R_u, which is not directly connected with the electrode reaction, was slightly larger compared to the reaction resistances, R_{ct} and R_W.

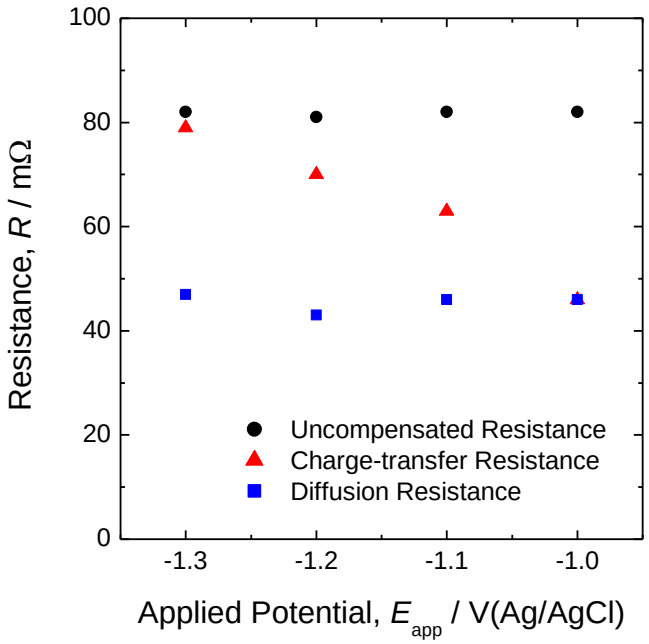

Figure 5. Plots of the uncompensated ohmic resistance R_u, charge transfer resistance R_{ct}, and diffusion resistance R_W against the applied potential, determined from the complex nonlinear least squares (CNLS) fitting of the experimental impedance spectra of Fig. 4(a) to the equivalent circuit of Fig. 4(b).

Since the potentiostatic current transient technique is helpful to elucidate reaction mechanisms [20,21], we used it to specify the rate-determining step for the U dissolution reaction. Fig. 6 shows the

anodic current transients on a logarithmic scale, which were experimentally measured on the U pellet electrode by applying a potential jump from the OCP to various applied potentials ranging from -1.3 to 1.0 V (Ag/AgCl). Herein, the current was previously corrected with a steady-state current I_{st} assuming first-order kinetics. As shown in Fig. 6, the current decreased monotonically in all the curves, but the relationship between the current transients and time on a logarithmic scale was not linear, except in the early stage with an absolute slope of 0.5. This abnormality can be attributed to the uncompensated ohmic potential drop. It has already been shown that in the presence of a large ohmic potential drop across an electrolyte, the current transient deviates from the linear relationship between log I-I_{st} and log t with an absolute slope of 0.5 [22,23]. While the current transient is easily influenced by the ohmic potential drop, the impedance spectrum is hardly affected by the uncompensated ohmic potential drop. Thus, it is concluded that a potentiostatic current transient method is not useful to investigate the kinetic behavior in the case of a large ohmic potential drop.

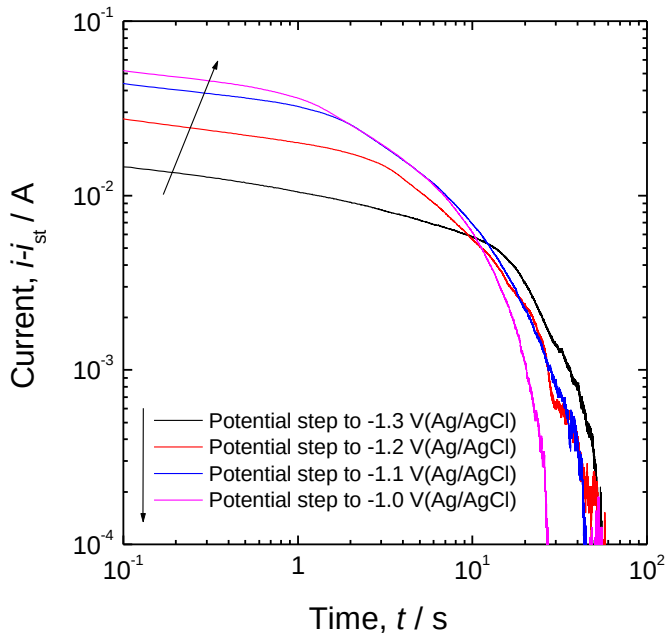

Figure 6. Anodic current transients on a logarithmic scale experimentally measured on the U pellet electrode by applying anodic potential jumps from the open-circuit potential (OCP) to various applied potentials from -1.3 to -1.0 V (Ag/AgCl).

3.3. Determination of kinetic parameters from AC impedance spectra

As mentioned in Section 3.2, the pure charge-transfer resistance can be obtained by employing AC-impedance spectroscopy. In this respect, we can determine the kinetic parameters more precisely by the values from the impedance spectra. At first, the exchange current density can be calculated from

the linear relationship between the electrode potential and the logarithmic charge-transfer resistance, as shown in Fig. 7, as follows:

$$R_{\mathrm{ct}}\big|_{\eta=0} = R_p = \frac{RT}{zFi_o} \tag{6}$$

The charge-transfer resistance at η = 0 is the same as the polarization resistance of the dissolution reaction. Using Eq. (6), the values of i_o was calculated to be 7.59×10^{-2} A cm^{-2} by taking the values of R_{ct} at η = 0 as 82.96 mΩ.

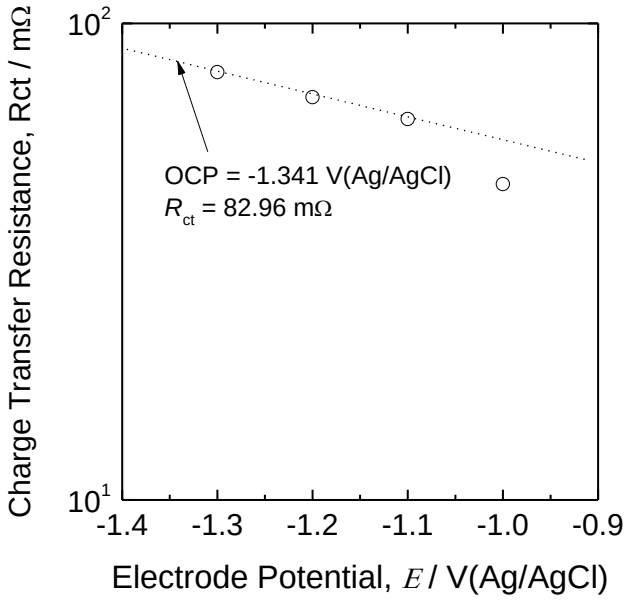

Figure 7. Change in the charge transfer resistance R_{ct} with the logarithm of the electrode potential from the values of Fig. 5.

4. CONCLUSION

In this work, the kinetics of uranium dissolution at the anode during the electrorefining process was investigated using various electrochemical methods such as potentiodynamic polarization method and AC impedance spectroscopy. The results are summarized as follows:

1. The kinetic parameters governing the U dissolution reaction can be easily determined by employing electrochemical methods. From the analyses of the polarization curve and potential transient, the exchange current density for U dissolution and diffusivity of U ions through the electrolyte were uniquely determined.

2. From the analysis of the impedance spectra obtained at various applied potentials, the uranium dissolution proceeds under a condition in which the interfacial charge transfer is kinetically

coupled with the diffusion through the electrolyte. In addition, the effect of the diffusion resistance on the dissolution resistance increased with an increase in the overpotential.

3. From the results of the current transient, it was shown that large value of uncompensated ohmic resistance interferes with investigations of kinetic behaviors, and hence AC-impedance spectroscopy is a more useful tool for kinetic studies in the presence of a large uncompensated ohmic potential drop.

ACKNOWLEDGEMENTS
This work was supported by a National Research Foundation of Korea (NRF) grant funded by the Korean government (MSIP) (No.2017M2A8A5015079).

References

1. Z. Tomczuk, J. P. Ackerman, R. D. Wolson and W. E. Miller, *J. Electrochem. Soc.*, 139 (1992) 3523.
2. J. L. Willit, W. E. Miller and J. E. Battles, *J. Nucl. Mater.*, 195 (1992) 229.
3. J. J. Laidler, J. E. Battles, W. E. Miller, J. P. Ackerman and E. L. Carls, *Prog. Nucl. Energy.*, 31 (1996) 131.
4. M. Iizuka, Y. Sakamura and T. Inoue, *Nucl. Eng. Technol*., 40 (2008) 183.
5. K. M. Goff, J. C. Wass, K. C. Marsden and G. M. Teske, *Nucl. Eng. Technol*., 43 (2011) 335.
6. M. Iizuka, K. Uozumi, T. Ogata, T. Omori and T. Tsukada, *J. Nucl. Sci. Technol.*, 46 (2009) 699.
7. J. H. Lee, Y. H. Kang, S. C. Hwang, J. B. Shim, B. G. Ahn, E. H. Kim and S. W. Park, *J. Nucl. Sci Technol.*, 43 (2006) 263.
8. F. Gao, C. Wang, L. Liu, J. Guo, S. Chang, L. Chang, R. Li and Y. Ouyang, *J. Radioanal. Nucl. Chem.*, 280 (2009) 207.
9. T. C. Totemeier and R. D. Mariani, *J. Nucl. Mater.*, 250 (1997) 131.
10. S. X. Li, Anodic Process of Electrorefining Spent Nuclear Fuel in Molten LiCl-KCl-UCl_3/Cd System, Proceedings of the 201st Meeting of the Electrochemical Society, Molten Salts XIII, Philadelphia, PA, USA, 2002, 541.
11. D. A. Jones, Principles and Prevention of Corrosion, second ed., Prentice Hall, (1996) Upper Saddle River, NJ, USA.
12. A. J. Bard and L. R. Faulkner, Electrochemical Methods - Fundamentals and Application, second ed., John Wiley & Sons, (2001) New York, USA.
13. J. Zhang, *J. Nucl. Mater.*, 447 (2014) 271.
14. R. O. Hoover, M. R. Shaltry, S. Martin, K. Sridharan and S. Phongikaroon, *J. Nucl. Mater.*, 452 (2014) 389.
15. E. Barsoukov and J. R. Macdonald, Impedance Spectroscopy – Theory, Experiment, and Applications, John Wiley & Sons, (2005) Hoboken, NJ, USA.
16. G. Y. Kim, D. Yoon, S. Paek, S. H. Kim, T. J. Kim and D. H. Ahn, *J. Electroanal. Chem.*, 682 (2012) 128.
17. D. Malevich, E. Halliop, B. A. Peppley, J. G. Pharoah and K. Karan, *J. Electrochem. Soc.*, 156 (2009) B216.
18. S. E. Chun, S. I. Pyun and G. J. Lee, *Electrochim. Acta.*, 51 (2006) 6479.
19. X. Ge, C. Fu and S.H. Chan, *Phys. Chem. Chem. Phys.*, 13 (2011) 15134.
20. S. J. Lee, S. I. Pyun and J. W. Lee, *Electrochim. Acta.*, 50 (2005) 1121.
21. S. J. Lee and S. I. Pyun, *Electrochim. Acta.*, 52 (2007) 6525.

22. J. N. Han, M. Seo and S. I. Pyun, *J. Electroanal. Chem.*, 499 (2001) 152.
23. J. W. Lee and S.I. Pyun, *Electrochim. Acta.*, 50 (2005) 1777.